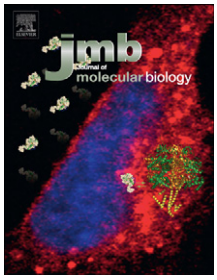

Yeast Rvb1 and Rvb2 Proteins Oligomerize As a Conformationally Variable Dodecamer with Low Frequency

Ajitha Jeganathan[1], Vivian Leong[1], Liang Zhao[2], Jennifer Huen[2], Nardin Nano[2], Walid A. Houry[2] and Joaquin Ortega[1]

1 - Department of Biochemistry and Biomedical Sciences and Michael G. DeGroote Institute for Infectious Diseases Research, *McMaster University, 1280 Main Street West, Hamilton, Ontario, Canada L8S 4K1*
2 - Department of Biochemistry, *University of Toronto, Toronto, Ontario, Canada M5S 1A8*

Correspondence to Joaquin Ortega: *Department of Biochemistry and Biomedical Sciences and Michael G. DeGroote Institute for Infectious Diseases Research, Health Sciences Centre, Room 4H24, McMaster University, 1280 Main Street West, Hamilton, Ontario, Canada L8S 4K1. Fax: +1 905 522 9033. ortegaj@mcmaster.ca*
http://dx.doi.org/10.1016/j.jmb.2015.01.010
Edited by T. Yeates

Abstract

Rvb1 and Rvb2 are conserved AAA+ (*A*TPases *a*ssociated with diverse cellular *a*ctivities) proteins found at the core of large multicomponent complexes that play key roles in chromatin remodeling, integrity of the telomeres, ribonucleoprotein complex biogenesis and other essential cellular processes. These proteins contain an AAA+ domain for ATP binding and hydrolysis and an insertion domain proposed to bind DNA/RNA. Yeast Rvb1 and Rvb2 proteins oligomerize primarily as heterohexameric rings. The six AAA+ core domains form the body of the ring and the insertion domains protrude from one face of the ring. Conversely, human Rvbs form a mixture of hexamers and dodecamers made of two stacked hexamers interacting through the insertion domains. Human dodecamers adopt either a contracted or a stretched conformation. Here, we found that yeast Rvb1/Rvb2 complexes when assembled *in vivo* mainly form hexamers but they also assemble as dodecamers with a frequency lower than 10%. Yeast dodecamers adopt not only the stretched and contracted structures that have been described for human Rvb1/Rvb2 dodecamers but also intermediate conformations in between these two extreme states. The orientation of the insertion domains of Rvb1 and Rvb2 proteins in these conformers changes as the dodecamer transitions from the stretched structure to a more contracted structure. Finally, we observed that for the yeast proteins, oligomerization as a dodecamer inhibits the ATPase activity of the Rvb1/Rvb2 complex. These results indicate that although human and yeast Rvb1 and Rvb2 proteins share high degree of homology, there are significant differences in their oligomeric behavior and dynamics.

Communication

Rvb1 and Rvb2 are highly conserved eukaryotic AAA+ (*A*TPases *a*ssociated with diverse cellular *a*ctivities) proteins that are essential in *Saccharomyces cerevisiae* [1], *Drosophila melanogaster* [2] and *Caenorhabditis elegans* [3]. They are also important for embryogenesis and early development in animals. For example, knockdown of Rvb1 in hematopoietic stem cells results in loss of pluripotency and Rvb1 null embryos do not pass the blastocyst stage [4].

The Rvbs were first found as part of the large RNA polymerase II holoenzyme and thought to act as a helicase able to unwind DNA and RNA [1]. However, they also play key roles in other essential cellular processes that do not require the helicase activity. These processes include chromatin remodeling [5–8], ribonucleoprotein complex biogenesis [9–11], transcription regulation [7,12], integrity of the telomeres [12], RNA polymerase II assembly [13] and phosphatidylinositol 3-kinase-related protein kinase signaling [14]. It has been proposed that the function the Rvb proteins perform in complexes mediating these processes is that of a chaperone. In these cases, the Rvbs constitutively or transiently associate with the assembling complexes and either assist in

recruitment of proteins, DNA and RNA components, or facilitate their interactions [3].

The structure and oligomeric state adopted by the Rvbs in both the isolated form and as part of larger multicomponent complexes that mediate these cellular processes has been a subject of intensive studies by several groups [15–19]. Initial X-ray crystallography studies with purified human Rvb1 protein [18] showed that this protein assembles into hexameric rings (Fig. 1b), which is typical of AAA+ proteins. Each protomer in the hexameric ring features three regions: DI, DII and DIII. The first and the last fragments make up the AAA+ core that includes the conserved sequences of the AAA+ module essential for ATP binding and hydrolysis (Walker A, Walker B, sensor 1 and sensor 2 motifs). DII, also known as the insertion domain, is a 170-amino-acid stretch proposed to bind DNA/RNA and that attaches to DI and DIII by a linker region folded as two β-strands (Fig. 1a). Subsequently, other groups have reported X-ray [16] and EM (*e*lectron *m*icroscopy) [17] structures of purified human Rvb1/Rvb2 complexes. A crystal structure with a DII truncation in both human Rvb1 and Rvb2 [16] (Fig. 1c) showed that the human proteins assemble into a barrel-shaped dodecamer composed of two stacked hexameric rings made of alternating Rvb1 and Rvb2 subunits. The interaction between the two rings occurs through the remaining part of the DII domain, still present in the Rvb1 and Rvb2 constructs, which occupies the equatorial part of the barrel. The AAA+ core domains of the hexamers are located at the ends of the barrel. A cryo-EM structure [17] was produced with full-length human Rvb1 and Rvb2 proteins and this structure was also consistent with the Rvb1/Rvb2 complex adopting a double hexameric ring structure. Nevertheless, these double ring structures formed by the human Rvb1/Rvb2 complex coexist in solution with single hexameric rings as demonstrated by size-exclusion chromatography [17] and analytical centrifugation analysis [20].

In the case of the yeast Rvb proteins, previous studies [15,21] showed that purified and *in vitro* assembled Rvb1/Rvb2 complexes exclusively form hexameric rings. However, the presence of an N-terminal histidine tag in yeast Rvb1 or Rvb2 induces the formation of double hexameric ring structures [19,22]. Recently, the structures of the yeast SWR1 [23] and INO80 [24] chromatin-

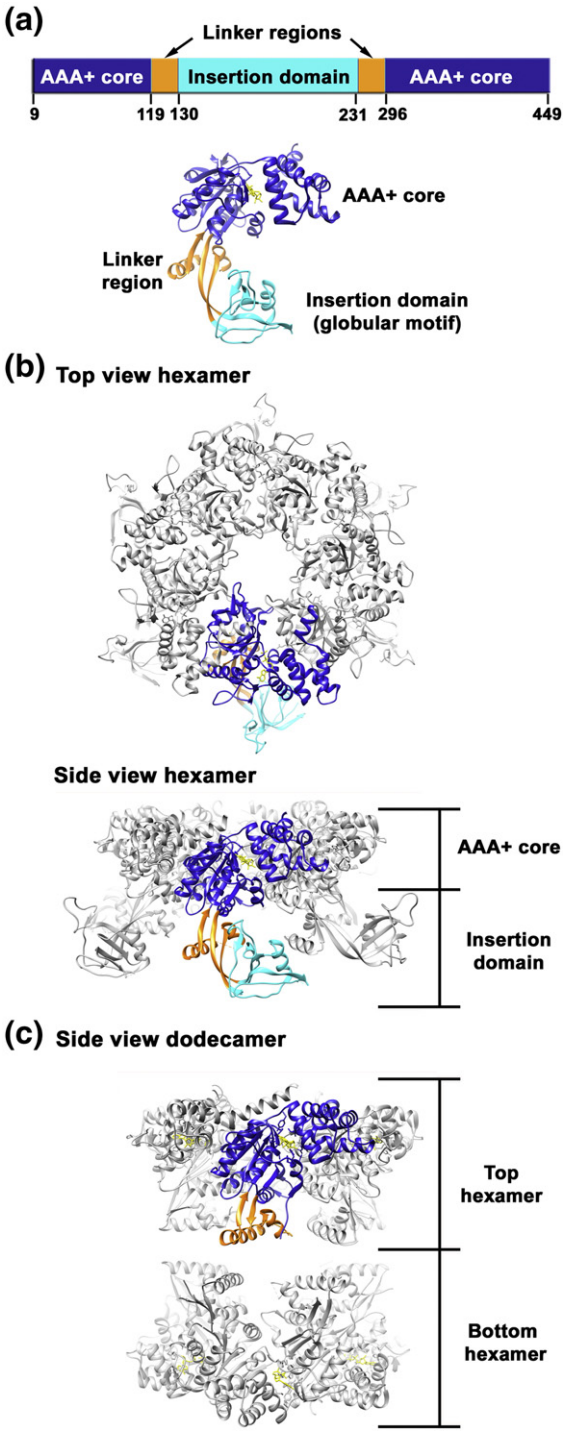

Fig. 1. X-ray structures of the hexamer and dodecamer formed by the human Rvb proteins. (a) The linear diagram in the top panel indicates the location of the domains of the human Rvb1 protein. The numbers correspond to the residues delimiting the domains. The ribbon representation of the human Rvb1 protein is shown in the bottom panel with domains colored as in the linear diagram. (b) Top and side views of the crystal structure of the hexamer formed by human Rvb1 protein. One of the protomers shows the protein domains colored as in the linear diagram. Structures in (a) and (b) were prepared using PDB ID 2C9O. (c) Side view of the human dodecameric Rvb1/Rvb2 complex obtained by X-ray crystallography (PDB ID 2XSZ). The Rvb1 and Rvb2 variants used to produce this structure had a truncation removing most of the insertion domain.

remodeling complexes have been obtained by cryo-EM. These complexes catalyze the swapping of the H2A.Z histone variant into the canonical H2A/H2B histone dimers in the nucleosome. This is an important chromatin remodeling mechanism through which cells regulate transcription, replication, cell division and DNA repair [8,25,26]. The SWR1 and INO80 complexes are composed of 14 [27] and 15 [8] different protein components, respectively. Several of the polypeptides forming these complexes, including the Rvb1 and Rvb2, are shared. However, the structures of the SWR1 and INO80 complexes are different. The SWR1 complex has a compact architecture, where Rvb1 and Rvb2 proteins form a single heterohexameric ring occupying the base of the complex [23]. The cryo-EM structure of the INO80 complex shows an embryo-shaped architecture with multiple domains (head, neck, body and foot) [24]. In this case, a Rvb1/Rvb2 heterododecamer of architecture similar to those described for the human Rvb1/Rvb2 complex occupies the head domain of the complex. The differences in the assembly of Rvb1/Rvb2 in these two complexes illustrate that the ability of the Rvb proteins to assemble as single or double hexameric rings is shared by both human and yeast proteins. However, it is possible that the type of complex in which they are found determines the oligomeric state adopted by the Rvbs.

In addition to the ability of the Rvb1/Rvb2 complex to oligomerize as both a hexamer and as a dodecamer, the ability to adopt multiple conformations is also an inherent characteristic of these complexes. Recently, a cryo-EM study [17] reported that the double ring structure formed by the purified human Rvb1/Rvb2 complex can adopt either a contracted or a stretched configuration differing in the orientation of the insertion domains. The movement of these domains causes the

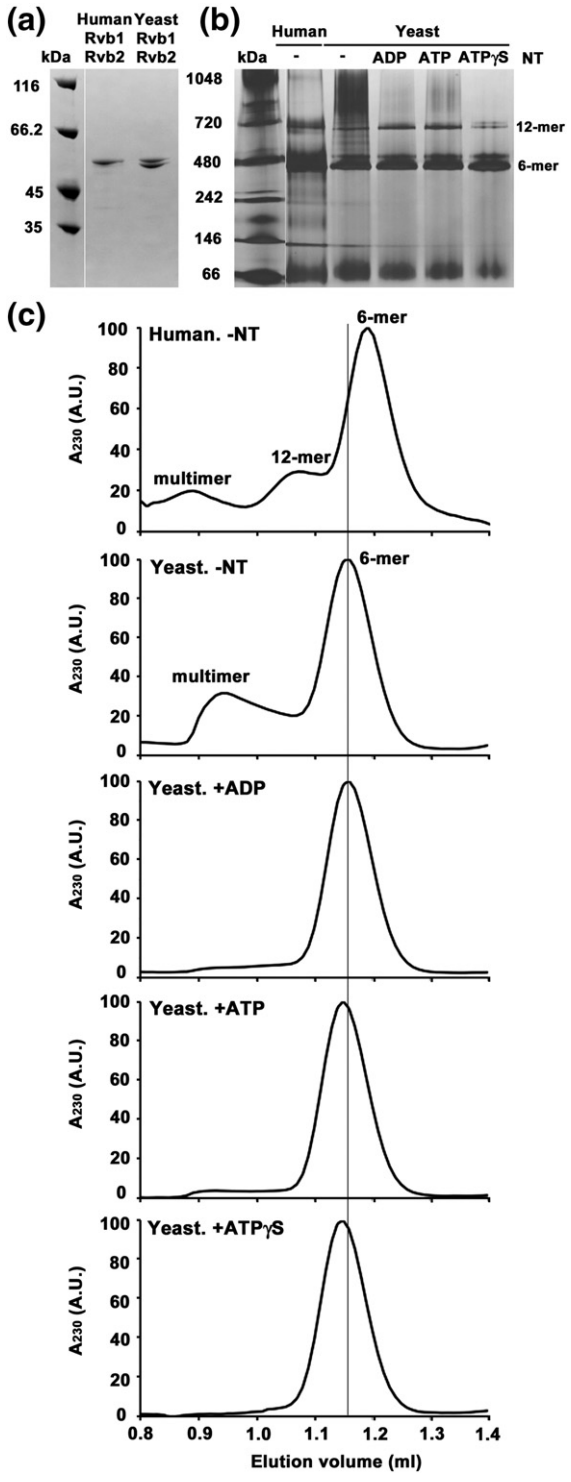

Fig. 2. Oligomeric state of the *in vivo* assembled yeast Rvb1/Rvb2 complexes. (a) Purified human and *in vivo* assembled yeast Rvb1/Rvb2 complexes resolved on a 12% SDS-PAGE gel and stained by Coomassie brilliant blue. (b) Human and yeast Rvb1/Rvb2 complexes were diluted in buffer containing 25 mM Tris–HCl (pH 7.5), 80 mM KCl, 10% (vol/vol) glycerol and 1 mM DTT. Total concentration of protomer was 6 μM and the concentration of the nucleotide in the indicated reactions was 1.5 mM. Prior to loading, we incubated the samples at 37 °C for 30 min and then diluted them 4-fold in the same buffer. A volume of 15 μL of protein sample was mixed with 5 μL of sample loading dye and resolved in Blue native PAGE (NativePAGETM Novex® Bis-Tris Gel System; Invitrogen). (c) A 30-μL reaction with 24 μg of purified yeast Rvb1/Rvb2 complex was incubated in buffer containing 50 mM Tris–HCl (pH 7.5), 150 mM NaCl, 80 mM KCl, 10% glycerol (vol/vol) and 1 mM DTT for 30 min at 37 °C. In the case of the control sample containing human Rvb1/Rvb2 complexes, the 30-μL reaction was obtained by mixing 12 μg of each Rvb protein in the same buffer and incubating it under the same conditions. Where indicated, the specified nucleotide was added to a final concentration of 1.5 mM at the beginning of the incubation. Reactions mixtures were centrifuged at 10,000*g* for 10 min and then injected (10 μL) into a Superdex 200 PC 3.2/30 on an AKTAmicro System (GE Healthcare Life Sciences) previously equilibrated in the same buffer at room temperature.

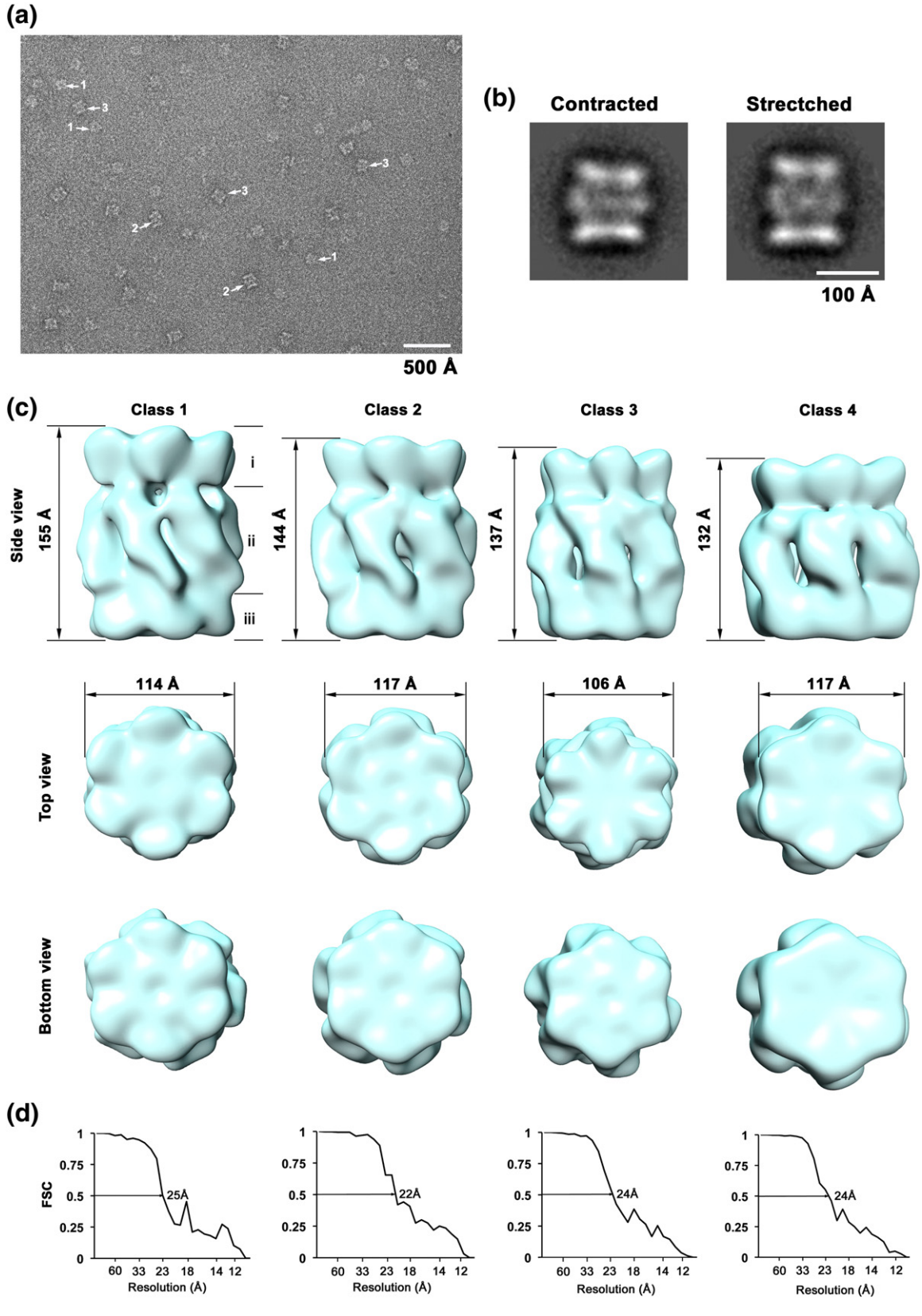
(a)
1
3
1
3
3
2
1
2
500 Å
(b)
Contracted
Strectched
100 Å
(c)
Class 1
Class 2
Class 3
Class 4
Side view
155 Å
144 Å
137 Å
132 Å
i
ii
iii
114 Å
117 Å
106 Å
117 Å
Top view
Bottom view
(d)
FSC
1
0.75
0.5
0.25
0
25Å
22Å
24Å
24Å
60 33 23 18 14 12
Resolution (Å)

complex to have different heights and changes the exposure of the putative DNA binding regions in the insertion domain (DII). However, the functional implications of this conformational variability observed in the dodecameric form of the human Rvb1/Rvb2 are not understood.

Here, we found that ~8% of *in vivo* assembled yeast Rvb1/Rvb2 complexes exist as double hexameric ring structures capable of adopting stretched and contracted conformations similar to the human Rvb1/Rvb2 complex. However, the yeast dodecamers also showed intermediate conformations, in which the structures displayed different degrees of contraction between the stretched and contracted states. The obtained structures revealed that the orientations of the insertion domains in the yeast dodecameric complexes were different from those observed in the contracted or stretched human structures. Finally, we show that oligomerization of the Rvb1 and Rvb2 proteins into a dodecamer inhibited the ATPase activity of the complex.

Consistent with our previous work [22], these results confirm that purified yeast Rvb1/Rvb2 complexes mainly exist as hexamers. They also highlight important differences between the human and yeast Rvb proteins in spite of their high degree of homology. Furthermore, this study reveals that the yeast Rvb1/Rvb2 complex is a very dynamic assembly capable of adopting oligomeric states and conformations similar to its counterpart in humans. The dynamic nature of these complexes is most likely essential for Rvb1/Rvb2 to carry out the diverse number of functions that these proteins perform in cells [28].

A small proportion of *in vivo* assembled yeast Rvb1/Rvb2 complexes exist as a dodecamer

The coexpression and purification of the Rvb1/Rvb2 complex was carried out as previously described [29]. Briefly, Rvb1 with an N-terminal His_6 tag followed by the tobacco etch virus cut site (HV tag) and untagged Rvb2 were coexpressed using pCOLADuet-1 in BL21 (DE3) pRIL and were purified using Ni-NTA resin column. The N-terminal HV tag of Rvb1 was removed by tobacco etch virus protease. Subsequently, the Rvb1/Rvb2 complex was further purified on a Superdex 200 10/300 GL column (GE Healthcare Life Sciences).

The purified complex was visualized using SDS-PAGE (Fig. 2a) and the oligomeric state was analyzed using Blue native PAGE (Fig. 2b). The purified *in vivo* assembled yeast Rvb1/Rvb2 complex showed a prominent band that migrated similarly to the 480-kDa molecular mass marker and a thinner band with mobility at ~720-kDa marker. Our previous work [15,21] established that even though the theoretical molecular masses of the hexameric and dodecameric Rvb1/Rvb2 complexes are ~300 kDa and ~600 kDa, respectively, these two bands correspond to the single and double ring complexes. The mobilities of these oligomers were also similar to the single and double hexameric complexes formed by the human Rvb1/Rvb2 complex loaded in the same gel as a control. In addition, in the lanes containing the yeast Rvb1 and Rvb2 proteins, we observed a smear of high-molecular-weight bands corresponding to a heterogenous mixture of oligomers. Incubation of the purified Rvb1/Rvb2 complex with ADP, ATP or ATPγS for 30 min at 37 °C dramatically reduced the presence of higher-order-mass oligomers above the 720-kDa marker. However, it did not dramatically change the relative intensity of the bands representing the Rvb1/Rvb2 hexamers and dodecamers, except in the presence of ATPγS. Quantification of these bands by densitometry (performed with ImageJ program) showed that ~8% of the Rvb1 and Rvb2 proteins in these samples are present as dodecamers in the presence of ADP or ATP. This proportion decreased to ~3% when the buffer contained ATPγS.

Fig. 3. EM of the *in vivo* assembled yeast Rvb1/Rvb2 dodecamers. (a) Purified *in vivo* assembled yeast Rvb1/Rvb2 complexes observed by negative-staining EM. Particles indicated with number 1 represent top views of the complex. Side views of the Rvb1/Rvb2 dodecamers in the stretched and contracted (or partially contracted) conformations are indicated with numbers 2 and 3, respectively. The specimen was deposited in copper grids covered with a continuous layer of carbon and stained with 2% uranyl acetate. Grids were imaged in a JEOL 2010F electron microscope operated at 200 kV. Images were collected at a magnification of 50,000× with a dose of ~20 electrons per angstrom squared. Recording of the images was performed on Kodak SO-163 films that we scanned on a Nikon Super COOLSCAN 9000 ED at 6.35 μm/pixel and averaged two times to produce micrographs with a sampling of 2.54 Å/pixel. (b) Projection structures of the contracted and stretched conformation of the Rvb1/Rvb2 dodecamer obtained by classification using self-organizing algorithms [31]. (c) 3D structure of the multiple conformations adopted by the yeast Rvb1/Rvb2 dodecamer. The three layers of density presented by these maps are indicated as i, ii and iii. Particle images for the 3D reconstructions were picked with Boxer [33]. The contrast transfer function of the micrographs was estimated using CTFFIND3 [34] and corrected using Xmipp package (Scheres *et al.*, 2008) The 3D reconstructions were obtained using the projection-matching approach as implemented in Xmipp [35] after particles in the multiple conformations were separated using maximum-likelihood-based classification approaches [36,37]. (d) Fourier shell correlation plots for the 3D structures in (c). Each plot was calculated from two maps obtained for each conformation following the last cycle of refinement from the even- and odd-numbered particles. The resolution values reported used the FSC = 0.5 criterion. The obtained cryo-EM maps were low-pass filtered to these resolution values.

The oligomeric state of the *in vivo* assembled yeast Rvb1/Rvb2 complex was also analyzed by size-exclusion chromatography (Fig. 2c). Injecting the control specimen, the N-terminal histidine-tagged human Rvb1/Rvb2 complex, produced a profile plot consistent with previous studies [17]. There was a major peak centered at an elution volume of 1.2 mL, which corresponded to the hexameric complex, as well as two minor broader peaks at 1.07 mL and 0.89 mL, representing the dodecameric form and other higher-order oligomers, respectively. Injecting the yeast Rvb1/Rvb2 complex produced a large peak eluting slightly earlier (1.16 mL) than the peak representing hexameric human Rvb1/Rvb2 complex. There was also a smaller peak centered at 0.94 mL that corresponded to the high-order oligomers observed as a smear in the native gel (Fig. 2b). A distinctive peak centered around 1.07 mL representing the Rvb1/Rvb2 dodecamer was not observed with the yeast proteins. However, we found that the merging point of the peaks representing the multimers and hexamers was at the expected elution volume for the Rvb1/Rvb2 dodecamer, and at that elution volume, the A_{230} reading was above the baseline consistent with the small proportion of dodecamers present in this sample. Incubation of the complex with nucleotides changed the elution profile resulting in a decrease in the peak containing the higher-order-mass oligomers to decrease dramatically. However, this peak did not disappear completely in the case of ADP or ATP consistent with the existence of a small proportion of multimers and dodecamers in these samples. In the case of the sample containing ATPγS, the peak representing the multimers decreased even further consistent with the lower proportion of dodecamers in this sample compared to those in the presence of ADP or ATP. In addition, in the reaction containing ATPγS, the peak representing the hexamer also shifted slightly in agreement with the conformational change that the complex undergoes in the presence of this nucleotide [30]. These results indicate that *in vivo* assembled yeast Rvb1/Rvb2 complexes mainly oligomerize as hexamers but a small proportion of these proteins assemble as dodecamers.

The yeast Rvb1/Rvb2 dodecamer complex adopts multiple conformations

To visualize the dodecameric structures formed by yeast Rvb1/Rvb2 complex, we imaged the purified assembly by negative-staining EM (Fig. 3a). The micrograph showed a mixture of ring- and barrel-shaped particles. Previous studies established that the ring-shaped particles are single hexameric rings formed by the Rvb1 and Rvb2 proteins [15,21]. The barrel-shaped particles showed three parallel striations similar to those previously seen in the dodecameric structures formed by the histidine-tagged versions of the yeast Rvb1 and Rvb2 proteins [19,22].

An initial set of 600 barrel-shaped particles was selected and subjected to 2D (*2-d*imensional) analysis. Particles were first centered and aligned using reference free methods before classifying them using self-organizing algorithms as implemented in the Xmipp program [31,32]. We found that the length of the barrel-shaped particles in the class averages fell into two categories. The first group contained longer particles with a length of approximately ~155 Å and the second group included the shorter particles with a longitudinal dimension of ~132 Å. Particle images assigned to these two groups were used to calculate a 2D projection structure of the two conformations that we called stretched and contracted, respectively (Fig. 3b), by analogy to the conformations observed in the human counterpart complex [17].

Unfortunately, visualizing the *in vivo* assembled Rvb1/Rvb2 complexes under non-staining conditions using cryo-EM failed to show any barrel-shaped particle (data not shown) indicating that either the dodecamers orient preferentially in the cryo-EM grids providing only end on views or that they were unable to withstand the vitrification process and dissociated into hexamers.

To further explore the conformational variability of the Rvb1/Rvb2 dodecamers and to obtain the 3D (*3-d*imensional) structure of the observed conformations, we selected 14,474 barrel-shaped particle images from the negative-staining electron micrographs and subjected them to maximum-likelihood-based classification (Scheres *et al.*, 2005b,c). This classification approach is an "unsupervised" method that does not require *a priori* information regarding the potential differences that may exist between particle images. Each group of particles obtained in the classification was used to obtain a 3D structure using projection-matching approaches [31,32]. Ring-shaped particles from the micrographs were not included in the data set to ensure that single hexameric ring Rvb1/Rvb2 complexes are not included in the 3D reconstruction process.

We found that there were four subpopulations of Rvb1/Rvb2 dodecamers present in the sample (Fig. 3c). The estimated resolution for the obtained 3D reconstructions ranged from 22 Å to 25 Å (Fig. 3d). Two of the 3D structures had a length of ~155 Å and ~132 Å and corresponded to the stretched and contracted Rvb1/Rvb2 dodecamers observed in the 2D analysis. The other two structures had a length of ~144 Å and ~137 Å and corresponded to partially contracted dodecamers with an intermediate length between the two extreme conformations initially observed. The percentages of particles from the stretched to the contracted structure were 12%, 28%, 43% and 17%, respectively. Performing

maximum-likelihood-based classifications assuming the existence of more than four subpopulations consistently produced duplication of the 3D structures displayed in Fig. 3c. Therefore, we concluded that the Rvb1/Rvb2 dodecamers mainly exist as four conformational subpopulations. It is possible that there were dodecamers with additional degrees of contraction; however our analysis suggests that these potential conformations may represent a very small percentage of the population. These results establish that the system has a continuous range of conformational stretching rather than adopting only two conformations

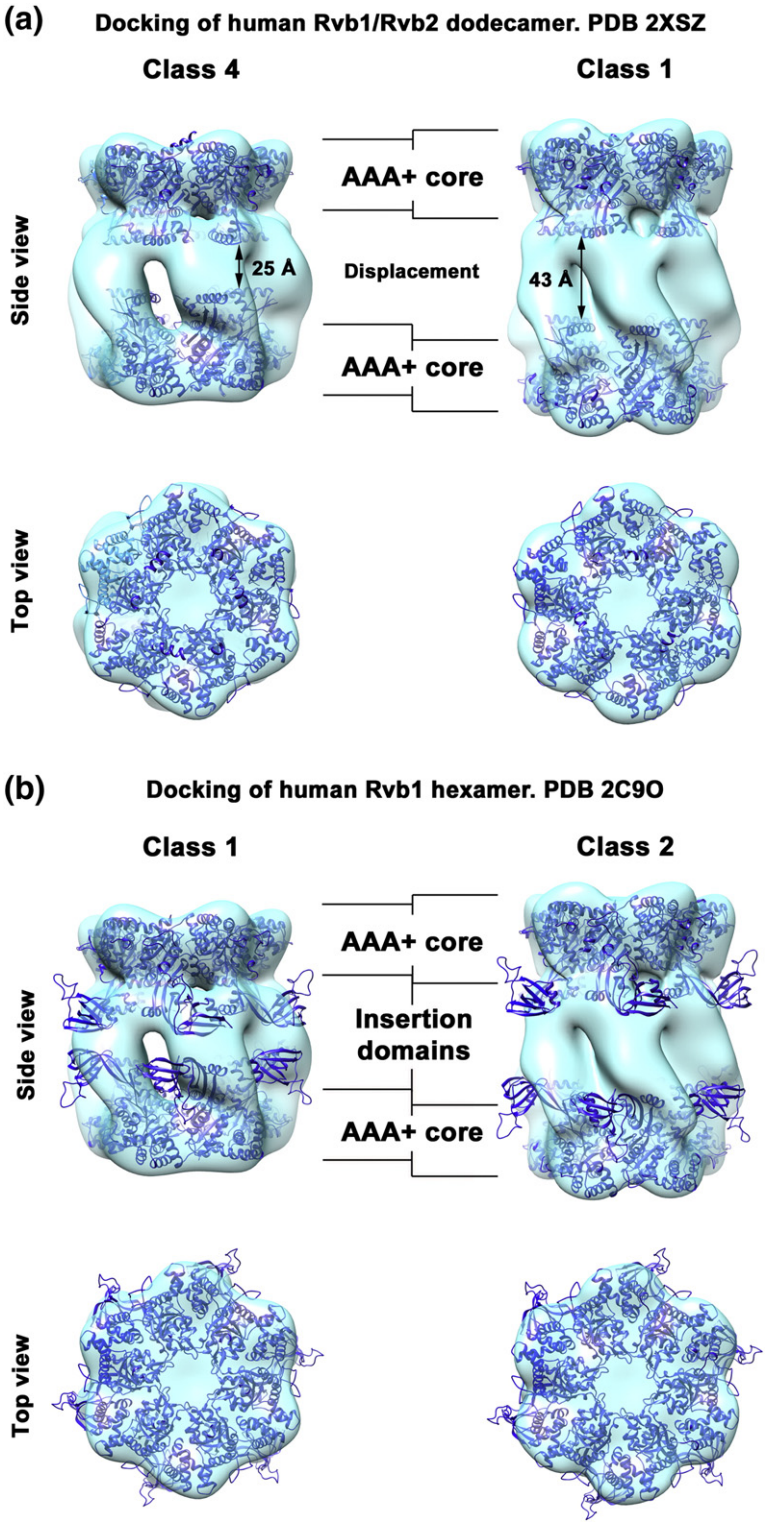

Fig. 4. Docking of the crystal structure of the human Rvb proteins into the EM maps of the *in vivo* assembled Rvb1/Rvb2 dodecamers in yeast. (a) Docking of the human Rvb1/Rvb2 dodecameric X-ray structure (Rvb1 and Rvb2 constructs lack the linker region and insertion domains; PDB ID 2XSZ) into two of the conformations [the most contracted (class 4) and the most stretched (class 1)] of the yeast Rvb1/Rvb2 dodecamers. Main domains of the Rvb proteins are indicated. The arrows in the side views indicate the distance between the remaining parts of the insertion domains in the X-ray structure after the two hexamers were fitted into the ends of the EM maps. (b) This panel shows the docking of the X-ray structure of the human Rvb1 hexamer (PDB ID 2C9O) into the same EM maps. Two hexamers were docked into each one of the EM maps. The Rvb1 protein in this structure contains the linker region and insertion domains.

as it has been described for the human Rvb1/Rvb2 dodecamers [17].

The obtained 3D structures (Fig. 3c) had the overall shape of a cylinder. In all cases, the cylinder consisted of two solid disks of density occupying the ends of the complex (Fig. 3c; indicated as i and iii) from where six densities projected meeting at the equator (Fig. 3c; indicated as ii). An interesting feature of the two 3D structures was that they did not show 2-fold symmetry with respect to an equatorial plane orthogonal to the longitudinal axis of the cylindrical structures. Consequently, in these structures, the top half was not identical to the bottom half and the densities projecting from the rings showed protrusions that were more prominent in the top than in the bottom part of the complex.

To ensure that the reconstructions were not affected by model bias, we refined each map twice using two reference structures that were aggressively low-pass filtered to 60 Å resolution. The two references used for the projection-matching refinements were the stretched 3D reconstruction of the human Rvb1/Rvb2 dodecameric complex (EMDB ID 2164) and the structure of the yeast dodecamer induced by the presence of N-terminal histidine tags in the Rvb1 and Rvb2 proteins (EMDB ID 5230). The two 3D structures obtained for each class were very similar, ruling out any model bias imposed by the references. The 6-fold symmetry around the longitudinal axis of the dodecamers was imposed during the 3D reconstruction procedures.

The Rvb1/Rvb2 dodecameric structures feature conformational variability in the insertion domain

To understand the conformational changes that the yeast Rvb1/Rvb2 dodecameric complex undergoes when it transitions between the different observed conformations, we fit the X-ray structures of the human Rvb1 hexamer and Rvb1/Rvb2 dodecamer into the most stretched and the most contracted of the obtained EM structures.

We first fit the X-ray structure of the human Rvb1/Rvb2 dodecamer (Fig. 4a). These fittings showed that the AAA+ core domains of the structure unambiguously fit in the outer rings of densities in the EM structures allowing us to assign the densities projecting from the rings to the insertion domains and linker regions of the Rvb1 and Rvb2 protomers. The length of EM structures was longer than the X-ray structure of the dodecamer. Therefore, optimal fitting of the X-ray structure of the dodecamer required pulling away the hexamers in the X-ray structure by different degrees. The X-ray structure of the human Rvb1/Rvb2 dodecamer was obtained with constructs of Rvb1 and Rvb2 lacking the linker region and insertion domains. Consequently, the EM density in the equatorial part of the EM maps was not filled by the X-ray structure. This slab of empty density was of 25 Å in the most contracted structure and up to 43 Å in the most stretched structure (Fig. 4a).

The X-ray structure of the human Rvb1 hexamer was produced with the full-length protein, and thus, we used this crystal structure to study the conformational differences in the insertion domain between the EM maps obtained for the Rvb1/Rvb2 dodecamer. Rigid-body fitting of two Rvb1 hexamers into the most stretched and the most contracted of the obtained EM structures (Fig. 4b) showed that the conformation of the linker region and insertion domain of the Rvb1 and Rvb2 protomers in the EM structures was different from that of the crystal structure. A large part of these two motifs extended outside the density of the EM maps, especially in the bottom part of the complexes that had smaller protrusions in the equatorial region. Consequently, part of the equatorial density of the EM maps remained unfilled upon docking of the X-ray structures. These results suggested that, in the EM structures, the insertion domains occupy a more inward position than that observed in the X-ray structure of the Rvb1 hexamer. In addition, they also indicated that the interaction between opposite hexamers in the EM dodecameric structures is mediated by protein/protein interactions involving the intermediate domains that contact each other at the equatorial part of the complex. Transition of the dodecamer from the stretched to any of the contracted structures most likely requires a conformational change of both the linker region and intermediate domains of the Rvb1 and Rvb2 protomer. Unfortunately, the limited

Table 1. ATPase activity of the hexameric and dodecameric form of the yeast Rvb1/Rvb2 complex.

Complex	Initial rate (pmol Pix min^{-1} × pmol Rvb^{-1})	Standard deviation
Rvb1/Rvb2	1.978	±0.197
Rvb1/H-Rvb2	1.469	±0.094
H-Rvb1/Rvb2	1.205	±0.088
H-Rvb1/H-Rvb2	0.768	±0.019
WB-Rvb1/WB-Rvb2	0.039	±0.009

Hydrolysis of ATP by 5 μM Rvb proteins (monomer) was monitored as a function of time by measuring the release of Pi by the malachite green assay. Assembly reactions were preincubated for 4 h at 4 °C prior to addition of 5 mM ATP. The reaction buffer contained 25 mM Tris–HCl (pH 7.5), 200 mM KCl, 5 mM $MgCl_2$, 1 mM DTT and 10% (vol/vol) glycerol. The reaction volume was 200 μL and samples were incubated at 37 °C. At the indicated time points, 10-μL samples were taken and added to 200 μL of reagent containing 1 mM malachite green, 8.5 mM ammonium molybdate and 1 M HCl to develop color. This reaction was stopped after 1 min by the addition of 25 μL of 37% citric acid and absorbance was measured at 660 nm. This reading was converted to picomoles of phosphate produced using a KH_2PO_4 standard curve. The initial rates were calculated from data collected in the first 10 min of the reactions. The prefix "H" indicates the protein containing a histidine tag. The prefix "WB" indicates that a Walker B variant of the Rvb1 and Rvb2 proteins was used in that reaction.

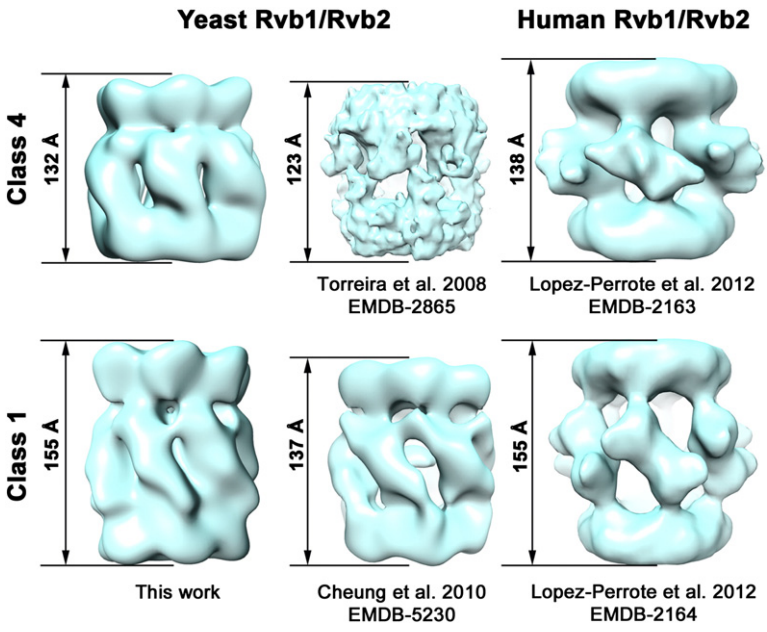

Fig. 5. Conformational variability of the human and yeast Rvb1/Rvb2 dodecamer. The EM structures of two of the conformations [the most contracted (class 4) and the most stretched (class 1)] conformations of the *in vivo* assembled Rvb1/Rvb2 complex from yeast described here are compared with previously obtained EM structures of the yeast and human dodecameric complex. The length of the complexes is indicated and each structure is labeled with the publication where the structure was described and their EMDB ID.

resolution of the EM structures prevented us from obtaining a detailed description of this conformational change.

Yeast Rvb1/Rvb2 dodecamers have decreased ATPase activity compared to hexamers

Yeast Rvb1 and Rvb2 are members of the AAA+ family of proteins and are active ATPases [19,30]. Here, we compared the ATPase activity of the dodecameric form of the complex with respect to that exhibited by the hexameric form. The small proportion of dodecamers present in our purified *in vivo* assembled Rvb1/Rvb2 complex prevented us from being able to biochemically separate the hexameric and dodecameric form before measuring their respective ATPase activities. We showed previously that N-terminal histidine tags on either Rvb1 or Rvb2 increased dodecamerization of the Rvb1/Rvb2 complex. This change in the oligomeric state is possibly caused by allosteric conformational changes within the insertion domain that favor ring/ring interactions. Therefore, we used N-terminal histidine variants of the Rvb1 and Rvb2 proteins to prepare samples with different proportions of hexamers and dodecamers [22] from which we measured the ATPase activity.

Initially, we assembled Rvb1/Rvb2 complexes *in vitro* by mixing equimolar amounts of Rvb1 and Rvb2 proteins. This assembly condition produced a sample mainly containing hexamers and only a small proportion of dodecamers [22], similar to the *in vivo* assembled yeast Rvb1/Rvb2 complexes analyzed here (Fig. 2). Subsequently, single histidine-tagged (H-Rvb1/Rvb2, Rvb1/H-Rvb2) and double histidine-tagged H-Rvb1/H-Rvb2 complexes were produced by substituting either one or the two proteins with the N-terminal histidine variant into the mixture. Mixtures containing the double histidine-tagged proteins produce a sample consisting mostly of dodecamers [22]. Replacing Rvb1 or Rvb2 with the histidine-tagged variant (H-Rvb1/Rvb2 and Rvb1/H-Rvb2 complexes) generated samples containing a mixture of hexamers and dodecamers [22].

Measuring the initial rates for ATP hydrolysis of these reactions showed that the activity was negatively correlated to the proportion of dodecamers present in the reaction (Table 1). The highest initial rates were obtained with the reaction containing the untagged Rvb proteins mainly composed of hexamers. Conversely, the mixture constituted mainly by dodecamers (H-Rvb1/H-Rvb2) gave the lowest initial rates. Reactions containing the single tagged complexes contained a mixture of hexamers and dodecamers and consequently exhibited initial rate values in between the samples made exclusively from hexamers and dodecamers. A reaction containing Walker B variants of Rvb1 (WB-Rvb1) and Rvb2 (WB-Rvb2) was used as a negative control and exhibited no significant ATPase. These results indicate that oligomerization of the Rvb1 and Rvb2 proteins into dodecameric complexes decreases their ATPase activity.

Concluding remarks

Previous work from our laboratory [22] showed that the presence of N-terminal histidine tags in the yeast Rvb1 and Rvb2 proteins promotes assembly as dodecamers instead of hexamers. We found that the height of these dodecamers (137 Å) induced by the presence of N-terminal histidine tags matches

one of the conformations (class 3) described here and it lies between that observed for the contracted conformation (132 Å) and that observed for the stretched conformation (155 Å) (Figs. 3 and 5). In addition, the structural features of the equatorial region containing the insertion and linker domains of the histidine-tagged Rvb variants are similar to the dodecameric structures described here, suggesting that they are in a similar conformation.

The contracted conformation obtained in this study was close in length to a previously described EM structure generated by coexpressing yeast Rvb1 and N-terminal histidine tag Rvb2 in insect cells [19]. However, comparison of the structures suggests some conformational differences in the insertion domains (Fig. 5).

Furthermore, the stretched and contracted structures that have been described for the human Rvb1/Rvb2 dodecameric complex [17] have 2-fold symmetry with respect to an equatorial plane orthogonal to the longitudinal axis of the cylindrical structures, which was not observed for the yeast complex. In addition, the insertion domains seem to be in a different conformation than the structure described in this study (Fig. 5).

Overall, the structures described in this study and their comparison with other published structures of dodecameric Rvb1/Rvb2 complexes suggest that this complex is extremely dynamic, especially in the linker region and insertion domains. This is likely a necessary requirement for this complex to participate in the assembly and functionality of a large number of macromolecular enzymes performing diverse essential activities in the cell. For example, recent cryo-EM work has provided the structure of the INO80 and SWR1 complexes and suggests that the Rvb1 and Rvb2 proteins oligomerize in these complexes as dodecamers and as hexamers, respectively. Our work presented here and previously published work [22,30] supports these two stoichiometries, as it shows that the dodecamers and as hexamers described for the Rvb1/Rvb2 module in the INO80 and SWR1 complexes can be adopted by the purified yeast Rvb1 and Rvb2 proteins.

In conclusion, this study reveals that the yeast Rvb1 and Rvb2 proteins assemble not only mainly as hexamers but also with low frequency as dodecamers that coexist in multiple conformations that differ in the orientation of their linker region and insertion domains. This work also indicates important differences between the yeast and human Rvb1 and Rvb2 proteins. Mainly that the dodecameric form in yeast is substantially less prevalent and that in addition to the stretched and contracted structures that have been described for human Rvb1/Rvb2 dodecamers, the yeast dodecamers also adopt intermediate conformations in between these two extreme states. It is possible that the human dodecamers also adopt intermediate conformations; however, those conformations have not been described. Nevertheless, any differences between the oligomeric behavior of the human and yeast Rvb1/Rvb2 complexes are surprising considering that the sequence identities between the insertion domains of yeast Rvb1 and Rvb2 and their human counterparts are >80%. This high level of identity implies that small differences in the amino acid sequence of this domain that mediates the interaction between the two hexamers in the dodecameric structure are sufficient to change the oligomeric behavior of the Rvb1 and Rvb2 proteins. Finally, we found that oligomerization as a dodecamer decreases the ATP hydrolysis rate of the complex. It is possible that the dodecameric form of the Rvb1/Rvb2 complex in yeast might be an inactive "storage" state that subsequently switches to an active hexameric state.

Accession numbers

The EM map for the multiple conformations of the yeast Rvb1/Rvb2 dodecamers have been deposited in the Electron Microscopy Data Bank and their ID numbers are EMDB IDs 6215, 6216, 6217 and 6218 for class 1, 2, 3 and 4, respectively.

Acknowledgements

We are grateful to the staff at the EM facility of the Faculty of Health Sciences and at Canadian Centre for Electron Microscopy at McMaster for their assistance with the electron microscope. J.H. was supported by a Natural Sciences and Engineering Research Council of Canada PGSD2 fellowship. This work was supported by a Canadian Institutes of Health Research grant (MOP-82930 to J.O. and MOP-93778 to W.A.H.). The funders had no role in study design, data collection and analysis, decision to publish or preparation of the manuscript.

Competing Financial Interest: The authors declare no competing financial interest.

Received 15 July 2014;
Received in revised form 16 December 2014;
Accepted 16 January 2015
Available online 28 January 2015

Keywords:
AAA+;
electron microscopy;
pontin;
reptin;
chromatin remodeling

References

[1] Qiu XB, Lin YL, Thome KC, Pian P, Schlegel BP, Weremowicz S, et al. An eukaryotic RuvB-like protein (RUVBL1) essential for growth. J Biol Chem 1998;273:27786–93.

[2] Bauer A, Chauvet S, Huber O, Usseglio F, Rothbacher U, Aragnol D, et al. Pontin52 and reptin52 function as antagonistic regulators of beta-catenin signalling activity. EMBO J 2000;19:6121–30.

[3] Nano N, Houry WA. Chaperone-like activity of the AAA+ proteins Rvb1 and Rvb2 in the assembly of various complexes. Philos Trans R Soc Lond B Biol Sci 2013;368:20110399.

[4] Bereshchenko O, Mancini E, Luciani L, Gambardella A, Riccardi C, Nerlov C. Pontin is essential for murine hematopoietic stem cell survival. Haematologica 2012;97:1291–4.

[5] Bakshi R, Mehta AK, Sharma R, Maiti S, Pasha S, Brahmachari V. Characterization of a human SWI2/SNF2 like protein hINO80: demonstration of catalytic and DNA binding activity. Biochem Biophys Res Commun 2006;339:313–20.

[6] Jin J, Cai Y, Yao T, Gottschalk AJ, Florens L, Swanson SK, et al. A mammalian chromatin remodeling complex with similarities to the yeast INO80 complex. J Biol Chem 2005;280:41207–12.

[7] Jonsson ZO, Dhar SK, Narlikar GJ, Auty R, Wagle N, Pellman D, et al. Rvb1p and Rvb2p are essential components of a chromatin remodeling complex that regulates transcription of over 5% of yeast genes. J Biol Chem 2001;276:16279–88.

[8] Shen X, Mizuguchi G, Hamiche A, Wu C. A chromatin remodelling complex involved in transcription and DNA processing. Nature 2000;406:541–4.

[9] McKeegan KS, Debieux CM, Boulon S, Bertrand E, Watkins NJ. A dynamic scaffold of pre-snoRNP factors facilitates human box C/D snoRNP assembly. Mol Cell Biol 2007;27:6782–93.

[10] McKeegan KS, Debieux CM, Watkins NJ. Evidence that the AAA+ proteins TIP48 and TIP49 bridge interactions between 15.5K and the related NOP56 and NOP58 proteins during box C/D snoRNP biogenesis. Mol Cell Biol 2009;29:4971–81.

[11] Zhao R, Kakihara Y, Gribun A, Huen J, Yang G, Khanna M, et al. Molecular chaperone Hsp90 stabilizes Pih1/Nop17 to maintain R2TP complex activity that regulates snoRNA accumulation. J Cell Biol 2008;180:563–78.

[12] Ohdate H, Lim CR, Kokubo T, Matsubara K, Kimata Y, Kohno K. Impairment of the DNA binding activity of the TATA-binding protein renders the transcriptional function of Rvb2p/Tih2p, the yeast RuvB-like protein, essential for cell growth. J Biol Chem 2003;278:14647–56.

[13] Boulon S, Marmier-Gourrier N, Pradet-Balade B, Wurth L, Verheggen C, Jady BE, et al. The Hsp90 chaperone controls the biogenesis of L7Ae RNPs through conserved machinery. J Cell Biol 2008;180:579–95.

[14] Izumi N, Yamashita A, Iwamatsu A, Kurata R, Nakamura H, Saari B, et al. AAA+ proteins RUVBL1 and RUVBL2 coordinate PIKK activity and function in nonsense-mediated mRNA decay. Sci Signal 2010;3:ra27.

[15] Cheung KL, Huen J, Houry WA, Ortega J. Comparison of the multiple oligomeric structures observed for the Rvb1 and Rvb2 proteins. Biochem Cell Biol 2010;88:77–88.

[16] Gorynia S, Bandeiras TM, Pinho FG, McVey CE, Vonrhein C, Round A, et al. Structural and functional insights into a dodecameric molecular machine—the RuvBL1/RuvBL2 complex. J Struct Biol 2011;176:279–91.

[17] Lopez-Perrote A, Munoz-Hernandez H, Gil D, Llorca O. Conformational transitions regulate the exposure of a DNA-binding domain in the RuvBL1-RuvBL2 complex. Nucleic Acids Res 2012;40:11086–99.

[18] Matias PM, Gorynia S, Donner P, Carrondo MA. Crystal structure of the human AAA+ protein RuvBL1. J Biol Chem 2006;281:38918–29.

[19] Torreira E, Jha S, Lopez-Blanco JR, Arias-Palomo E, Chacon P, Canas C, et al. Architecture of the pontin/reptin complex, essential in the assembly of several macromolecular complexes. Structure 2008;16:1511–20.

[20] Niewiarowski A, Bradley AS, Gor J, McKay AR, Perkins SJ, Tsaneva IR. Oligomeric assembly and interactions within the human RuvB-like RuvBL1 and RuvBL2 complexes. Biochem J 2010;429:113–25.

[21] Gribun A, Cheung KL, Huen J, Ortega J, Houry WA. Yeast Rvb1 and Rvb2 are ATP-dependent DNA helicases that form a heterohexameric complex. J Mol Biol 2008;376:1320–33.

[22] Cheung KL, Huen J, Kakihara Y, Houry WA, Ortega J. Alternative oligomeric states of the yeast Rvb1/Rvb2 complex induced by histidine tags. J Mol Biol 2010;404:478–92.

[23] Nguyen VQ, Ranjan A, Stengel F, Wei D, Aebersold R, Wu C, et al. Molecular architecture of the ATP-dependent chromatin-remodeling complex SWR1. Cell 2013;154:1220–31.

[24] Tosi A, Haas C, Herzog F, Gilmozzi A, Berninghausen O, Ungewickell C, et al. Structure and subunit topology of the INO80 chromatin remodeler and its nucleosome complex. Cell 2013;154:1207–19.

[25] Morrison AJ, Highland J, Krogan NJ, Arbel-Eden A, Greenblatt JF, Haber JE, et al. INO80 and gamma-H2AX interaction links ATP-dependent chromatin remodeling to DNA damage repair. Cell 2004;119:767–75.

[26] Papamichos-Chronakis M, Peterson CL. The Ino80 chromatin-remodeling enzyme regulates replisome function and stability. Nat Struct Mol Biol 2008;15:338–45.

[27] Wu WH, Alami S, Luk E, Wu CH, Sen S, Mizuguchi G, et al. Swc2 is a widely conserved H2AZ-binding module essential for ATP-dependent histone exchange. Nat Struct Mol Biol 2005;12:1064–71.

[28] Gerhold CB, Gasser SM. INO80 and SWR complexes: relating structure to function in chromatin remodeling. Trends Cell Biol 2014;24:619–31.

[29] Kakihara Y, Makhnevych T, Zhao L, Tang D, Houry WA. Nutritional status modulates box C/D snoRNP biogenesis by regulated subcellular relocalization of the R2TP complex. Genome Biol 2015 [in press].

[30] Gribun A, Kimber MS, Ching R, Sprangers R, Fiebig KM, Houry WA. The ClpP double ring tetradecameric protease exhibits plastic ring-ring interactions, and the N termini of its subunits form flexible loops that are essential for ClpXP and ClpAP complex formation. J Biol Chem 2005;280:16185–96.

[31] Scheres SH, Nunez-Ramirez R, Sorzano CO, Carazo JM, Marabini R. Image processing for electron microscopy single-particle analysis using XMIPP. Nat Protoc 2008;3:977–90.

[32] Sorzano CO, Marabini R, Velazquez-Muriel J, Bilbao-Castro JR, Scheres SH, Carazo JM, et al. XMIPP: a new generation of an open-source image processing package for electron microscopy. J Struct Biol 2004;148:194–204.

[33] Ludtke SJ, Baldwin PR, Chiu W. EMAN: semiautomated software for high-resolution single-particle reconstructions. J Struct Biol 1999;128:82–97.

[34] Mindell JA, Grigorieff N. Accurate determination of local defocus and specimen tilt in electron microscopy. J Struct Biol 2003;142:334–47.

[35] Scheres SH, Nunez-Ramirez R, Gomez-Llorente Y, San Martin C, Eggermont PP, Carazo JM. Modeling experimental image formation for likelihood-based classification of electron microscopy data. Structure 2007;15:1167–77.

[36] Scheres SH, Valle M, Carazo JM. Fast maximum-likelihood refinement of electron microscopy images. Bioinformatics 2005;21:ii243–4.

[37] Scheres SH, Valle M, Nunez R, Sorzano CO, Marabini R, Herman GT, et al. Maximum-likelihood multi-reference refinement for electron microscopy images. J Mol Biol 2005;348:139–49.